



ISSN: 0976-3031

Available Online at <http://www.recentscientific.com>

CODEN: IJRSFP (USA)

International Journal of Recent Scientific Research
Vol. 9, Issue, 2(I), pp. 24370-24380, February, 2018

**International Journal of
Recent Scientific
Research**

DOI: 10.24327/IJRSR

Research Article

DEVELOPMENT OF SUSTAINABLE DYE ADSORPTION SYSTEM USING NUTRACEUTICAL INDUSTRIAL TURMERIC ROOT SPENT- STUDIES WITH DIRECT RED 13

Mohammed A. H.Dhaif Allah¹ and Akheel Ahmed Syed*²

¹Department of Studies in Environmental Science, University of Mysore, Manasa Gangotri, Mysuru-570006, India

²Department of Studies in Chemistry, University of Mysore, Manasa Gangotri, Mysuru - 570006, India

DOI: <http://dx.doi.org/10.24327/ijrsr.2018.0902.1649>

ARTICLE INFO

Article History:

Received 18th November, 2017

Received in revised form 10th December, 2017

Accepted 06th January, 2018

Published online 28th February, 2018

Key Words:

Adsorption isotherms, ANOVA, Central composite design model, Direct Red 13, Kinetics, Nutraceutical industrial turmeric root spent, Pollution amelioration.

ABSTRACT

First-ever study on the removal of Direct Red 13 (DR13), a bis azo dye, extensively used in textile industry from aqueous media using inexpensive nutraceutical industrial turmeric root spent (NITRS) as a biosorbent is reported. The effects of various factors like initial dye concentration, adsorbent dosage and as also particle size, pH and temperature of media were studied. The experimental data collected under equilibrium conditions were analysed by two-parameter isotherm models of Langmuir, Freundlich and Tempkin. The pseudo-first order and pseudo-second order models were applied in adsorption kinetic studies. Kinetic data fitted well to pseudo-first order model. SEM images of NITRS depict high fibrous matrix with hierarchical porous structure. By FTIR analysis of the spent indicated the presence of cellulosic and ligno-cellulosic materials which impart hydrophilic and hydrophobic properties. The central composite experimental design (CCD) and the analysis of variance (ANOVA) indicated maximum DR13 adsorption of 23 mg/l by NITRS. The ANOVA also indicated the influence of each parameter and their combinations on the final adsorption capacity of the system. The investigation indicated that NITRS can be a cost-effective and a natural biosorbent for the remediation of toxic DR13 dye.

Copyright © Mohammed A. H.Dhaif Allah and Akheel Ahmed Syed, 2018, this is an open-access article distributed under the terms of the Creative Commons Attribution License, which permits unrestricted use, distribution and reproduction in any medium, provided the original work is properly cited.

INTRODUCTION

The ever-increasing population and living standard have created never-ending demand for textiles and clothing - one of the primary needs of human beings. The textile industry is globally the largest sector producing 60 billion kg fabric annually, using up to 9 trillion gallons of water (Zaffalon 2010). This massive water use is ultimately key component for creating pollution. Cutting down of water footprint and carbon footprint is an important concern for sustainable development of world's textile industry (Zaffalon 2010). Textile industry is one of the major consumers of dyes.

Azo dyes comprise about 70% of total world dye production and these are mainly used in textile industries (Bafana *et al.*, 2011; Hubbe *et al.*, 2011). The main problem with azo dyes is that they are discharged in large quantities to the environment as industrial effluents (Unnithan & Anirudhan 2001). The mixing of these pollutants with natural waters causes visible aesthetic colour problem even at low concentration, besides

causing serious health risks due to their toxicity to aquatic organisms and humans (Yao *et al.*, 1999). Azo dyes are highly stable in the environment owing to their resistance to natural oxidation and reduction, light exposure and biodegradation. Direct Red 13 (DR13), a bis azo dye is mainly used in cotton and glue dyeing and printing; silk, polyamide, viscose/polyamide fibre blended fabric dyeing and also extensively used to colour the paper and leather.

The nutraceutical sector is fast growing and according to Transparency Market Research global nutraceutical market should reach \$285.0 billion by 2021 from \$198.7 billion in 2016 at a compound annual growth rate of 7.5%, from 2016 to 2021 (globenewswire.com). The challenge faced by the nutraceutical industry is in handling waste which generates 50-95% of the total amount of the herbs, shrubs, seeds and/or roots processed to recover the active ingredient(s).

Turmeric (*Curcuma longa L.*) is a perennial herb originating from the rhizome of the plant *Curcuma longa L.* (Family:

*Corresponding author: Akheel Ahmed Syed

Department of Studies in Environmental Science, University of Mysore, Manasa Gangotri, Mysuru-570006, India

Zingiberaceae) and has a long history in Asia. The Indian Ayurveda medicine has used turmeric for curing several diseases since 1900 BC (Joe *et al.*, 2004). Turmeric contains curcumin as a prominent phenolic compound constituting 1–5% of turmeric and imparts the typical characteristic yellow colour. Curcumin has been the subject of hundreds of published papers over the past four decades, covering aspects like its antioxidant, anti-inflammatory, cancer chemopreventive and potentially chemotherapeutic properties (Sharma *et al.*, 2005). It is also used in drugs against dermatitis, AIDS and in high cholesterol level. Curcumin is also popular as a sunscreen lotion in cosmetic industry.

Biological, chemical and physical techniques, methods and procedures are reported for the remediation of azo dyes. Majority of the methods available are either expensive or associated with such problems as development of toxic intermediates, low removal efficiency and display higher specificity for some groups of dyes (Glenn *et al.*, 2014). Consequently, adsorption process is gaining greater importance due to its operational simplicity, commercial viability, process efficiency (Falkenmark 2003) and easy in scaling up of the process scale to field level (Unnithan & Anirudhan 2001). Any biosorbent to become fit for remediation of dyes should have such characteristics as that it should be available in plenty and also of low cost; it should not have any or minimal alternative use(s) so that the price should not increase; it should be in readily usable not requiring any pre-chemical treatment; and its pore structure should be such that it should permit better adsorption.

One of the extensively used adsorbents for remediation of azo dyes is the activated carbon produced from the agriculture biomass. But it has such limitations; as combustion at high temperature, blocking of pores, hygroscopicity and prohibitive cost of the material. Besides, the processes used for producing activated carbon enhance carbon footprint. In order to handle the large volume of wastewater generated by the textile industries, it is advantageous to use such adsorbents which are low cost, ready-to-use and abundantly available.

The Nutraceutical Industrial Spent (NIS) available in abundance has almost all the qualities as adsorbent for bioremediation of dyes in waste waters and/or industrial effluents. The nutraceuticals are subjected to thermal, mechanical and chemical processes, during extraction of the principle component(s) and as such they need no further chemical processing before being used for remediation of dyes from waters and industrial effluents. This adds on to the advantage of reducing the E-factor (Sheldon 1992) a metric used for “greenness” of the process, which is defined as “ratio of the total weight of waste produced to the total weight of the product obtained” assumes paramount importance. This metric spur innovation and results in reduction of waste through the system of recycling. SEM studies have shown that NITRS has enough fibrous structure to trap moisture and reduce calorific value and increase the toxic gas emissions on burning. The same structure helps to enhance adsorption capacity of toxic dyes.

Reports on the adsorption of dyes using low-cost biological materials are available but much information is not available on

the reuse of resulting “sludge”. In this connection our research school is the first to evaluate NIS as adsorbents for the remediation of toxic dyes (Taquiet *et al.*, 2017; Papegowda and Syed 2017; Sulthana *et al.*, 2017) and NIS and dye adsorbed (sludge) as filler materials for the fabrication of thermoplastic and thermoset composites (Pashaei *et al.*, 2011; Syed & Syed 2016; Syed & Syed 2016a; Syed & Syed 2012; Syed *et al.*, 2011; Syed *et al.*, 2010; Syed *et al.*, 2010a; Syed *et al.*, 2009; Taqui *et al.*, 2017). Herein we report for the first time about the remediation of Direct Red 13 dye from water using NITRS as biosorbent to develop sustainable adsorption system.

MATERIALS AND METHODS

Materials

Direct Red 13 (DR13) dye is soluble in water and ethanol producing wine red and red color respectively. It is insoluble in many organic solvents. [C.I. = 22155; CAS registry number = 1937-35-5; chemical formula = $C_{32}H_{22}N_6Na_2O_7S_2$; molecular weight = 712.66; absorbance maximum (λ_{max}) = 503 nm]. The molecular structure of the dye is shown in Figure 1.

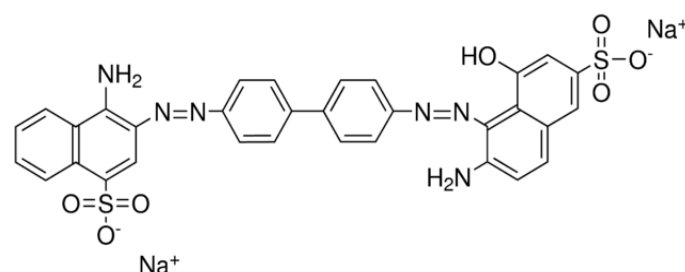


Figure 1 Structure of Direct Red 13

Adsorbent Preparation and Characterization

Adsorbent preparation

NITRS was collected obtained from a local factory and was dried in sunlight, crushed and ground using a ball mill and sieved as per ASTM standard particle sizes of ≤ 90 , $\geq 90 \leq 125$, $\geq 125 \leq 177$, $\geq 177 \leq 355$, $\geq 355 \leq 500$, $\geq 500 \leq 710$ μ .

Surface characterization

The surface morphology of the NITRS was visualized using an Electronic Microscope (LEO 435 VP model, Japan). The functional groups present in the adsorbent was identified by FTIR spectrometer (Inter-spec 2020, Spectro Lab, UK) measured the Infrared spectra of the control sample (NITRS before adsorption of DR13) and the DR13-loaded samples.

Batch adsorption experiments

Batch experiments were conducted with varying parameters. However, the common preliminary preparation involved the setting up of 250-ml flasks with 50 ml working aqueous solution of DR13 (100 mg L^{-1}). After the initial preparation, 50mg of NITRS were introduced into each flask. Temperature controlled shaker agitated the contents of the flasks at 165 rpm for 3h. Evaluations were conducted using the different parameters; which included varying dosage of NITRS (0.025, 0.050, 0.075, 0.100, 0.150, 0.200, 0.300 g); DR13 concentrations (25, 50, 75, 100, 125, 150, 175, 200, 300 and 400 mg L^{-1}), adsorbent particle size (≤ 90 , $\geq 90 \leq 125$, $\geq 125 \leq 177$, $\geq 177 \leq 355$, $\geq 355 \leq 500$, $\geq 500 \leq 710$ μ), pH (2, 4, 6, 7, 8, 10 and 12)

and temperature (303 K, 313 K and 323 K) constant dye concentration of 100ppm. The samples were centrifuged for 5 min to remove the leftover particulate matter. UV-Vis spectrophotometer (PerkinElmer-Lambda 25, USA) was used to measure the absorbance of the filtrate at 503 nm. Controls were maintained by using the adsorbent in distilled water and an adsorbent-free DR13.

Adsorption isotherms

Langmuir, Freundlich, and Tempkin are the widely accepted adsorption isotherm models for studying surface for single solute systems for the equilibrium adsorption at ambient temperature. Analysis was done on adsorption isotherms to describe the interaction between the adsorbate and adsorbent using the batch experimental data for the effect of initial DR13 concentration studies. The results of parameters in different models provide information on interaction mechanisms, surface properties and affinities of the adsorbent.

Adsorption kinetics

Erlenmeyer flasks were used for adsorption kinetics experiments. The flasks were populated with 50 mg of NITRS and 50 ml of DR13 solution of 100 pp mat (303K, 313K and 323K) temperatures and the readings were recorded, up to 180 min, when maximum adsorption capacity was almost reached. The experimental data were fit-in to the pseudo-first-order kinetic and pseudo-second-order kinetic models to find out the controlling mechanism involved in adsorption process.

Statistical optimization of process parameters

Six factors influencing the adsorption process on the final adsorption capacity were studied and these included: adsorption time (A), process temperature (B), initial dye concentration (C), Particle size (D) adsorbent dosage (E) and initial pH (F). These were the independent variables which were to be optimized for adsorption capacity which is the dependent response variable at fixed orbital shaking at 165 rpm. A standard experimental design was prepared comprising 6 factors at 2 levels (Table1). Analysis of variance was done on the results which yielded a general quadratic regression equation. Surface and contour plots were obtained which indicated graphically the effect of individual as well as interaction effects between parameters on the adsorption capacity.

Table 1 Experimental design of high and low levels of factors

Factor	Name	Units	Minimum	Maximum
A	Time	minute	0	180
B	Temperature	°C	27	50
C	Concentration	mg/L	25	400
D	Particle size	μ	90	710
E	Adsorbent dosage	g/L	0.025	0.3
F	pH		2	12

RESULTS AND DISCUSSION

Characterization of the adsorbent

Surface characterization

The surface characterization was perceived through SEM. The SEM image of NITRS displayed a slightly porous structure (Figure 2a). After adsorption it was observed that some of the pores were completely filled with the adsorbate(DR13) forming

a thin film over the particle (Figure 2b). An IR spectrum of NITRS provides the information about the functional groups present (Figures 3a, 3b and 3c). The IR absorption spectrum (Figure 3b) displayed a weak band between 3200-3300 cm⁻¹ is assigned to the hydroxyl groups of cellulose and adsorbed water molecule. Whereas, a broadband at 2250 cm⁻¹ is assigned to C-H symmetric stretching and a band at 1100 cm⁻¹ is due to the C-O-C stretching.

Figure 3c shows a broadband in the range 3000-3600 cm⁻¹. This is assigned to the hydroxyl groups of cellulose and adsorbed water molecule. The disappearance of the sharp peak of DR13 for NH₂, N-N, and S=O at 3000, 1400 and 1000 cm⁻¹ in DR13-NITRS spectrum confirms the strong adsorption of DR13 on NITRS.

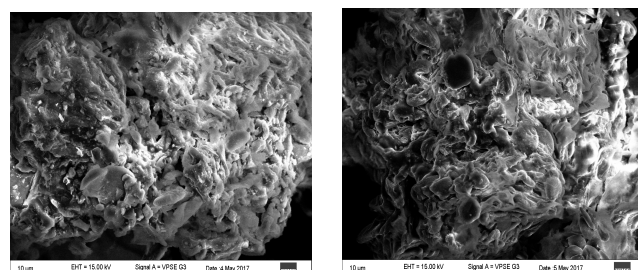


Figure 2a SEM image of NITRS **Figure 2b** SEM image of DR13-NITRS

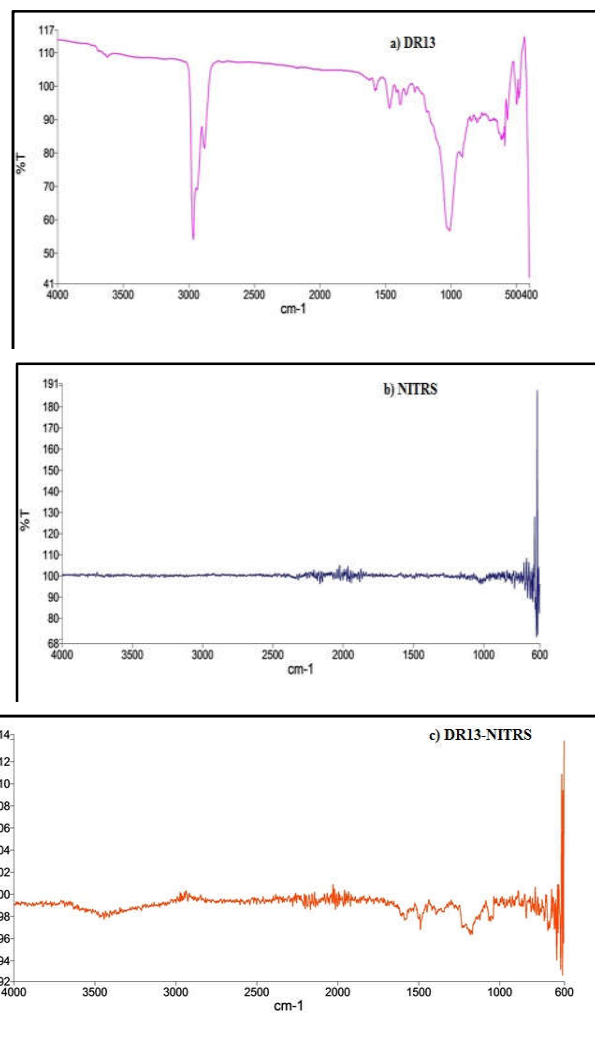


Figure 3 FTIR spectra of a) DR13, b) NITRS and c) DR13 adsorbed on NITRS

The finger print region of the biological material NITRS indicates complex bands and accurate assignment of the peaks without the help of standard sample is difficult. However, the presence of cellulose and lignin indicates that the spent possibly displays both hydrophilic and hydrophobic properties. In short, based on the disappearance of IR absorption frequencies, in Figure 3a, it is evident that to a large range DR13 has adsorbed on NITRS.

Batch Adsorption Studies

Effect of initial dye concentration and adsorbent dosage

In order to achieve maximum adsorption, it is necessary to determine the optimal parameters. The maximum adsorption capacity (q_e) of 23mg/g was reached for initial DR13 concentration of 100 mg/L (Figure 4a). There was an increase and then decrease in adsorbent dose at 50 mg g⁻¹ (Figure 4b). The results show that by choosing an appropriate dose of NITRS, it will be possible to remove maximum DR13 dye from the aqueous medium.

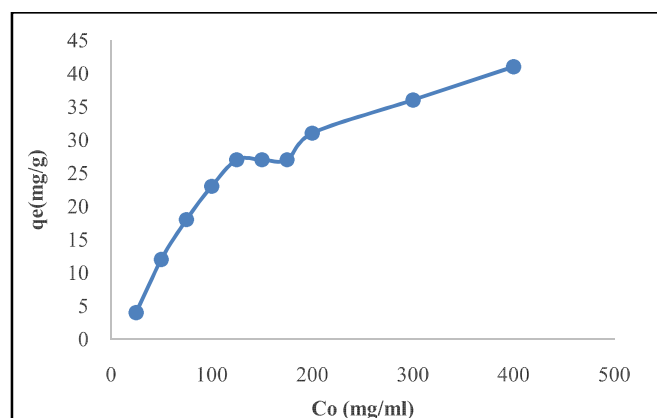


Figure 4a Effect of Initial dye concentration on dye adsorption

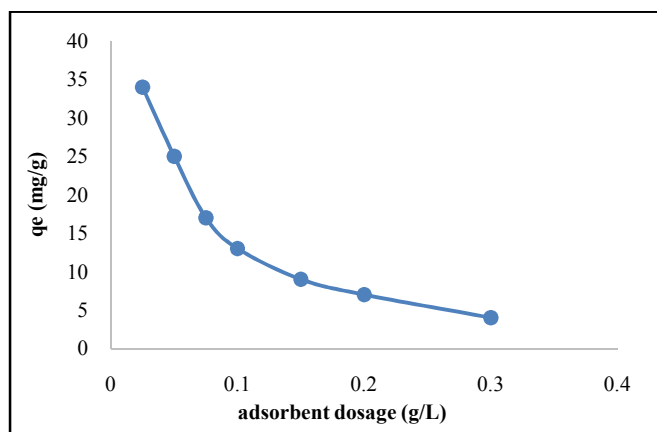


Figure 4 b Effect of adsorbent dosage on dye adsorption

Effect of Particle Size

Maximum adsorption capacity was studied with initial DR13 dye concentration of 100 mg/L at neutral pH. The experiment was performed with different particle sizes including $\leq 90 \mu\text{m}$; $\geq 90 \mu\text{m} \leq 125 \mu\text{m}$; $\geq 125 \mu\text{m} \leq 177 \mu\text{m}$; $\geq 177 \mu\text{m} \leq 355 \mu\text{m}$; $\geq 355 \mu\text{m} \leq 500 \mu\text{m}$ and $\geq 500 \mu\text{m} \leq 710 \mu\text{m}$. Adsorption of dye decrease with increase in size of the adsorbent particle. This is in conformation with the expected results as surface area decreases with increase in particle size. An optimum size

of $\geq 125 \mu\text{m}$ and $\leq 177 \mu\text{m}$ (80 mesh ASTM) was selected for the studies because of two reasons: first, 80 mesh particle is widely employed in the fabrication of composites and second, sieving lower size particles will take longer period and adds to the cost of the process. Maximum adsorption was observed with particle size of $\geq 125 \mu\text{m} \leq 177 \mu\text{m}$ (Figure 4c).

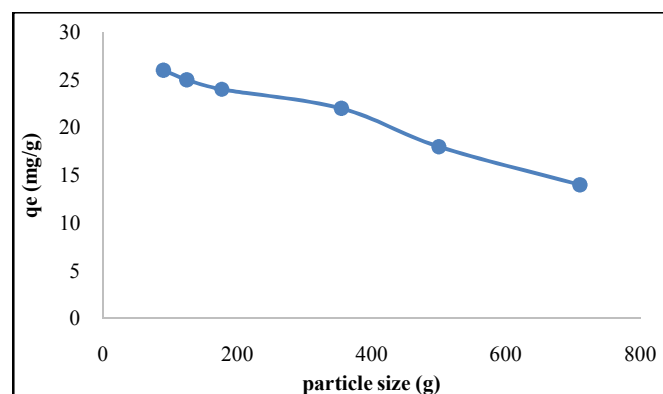


Figure 4 c Effect of particle size on dye adsorption

Effect of pH

Adsorption of the dye on to the adsorbent decreased almost exponentially as the pH increased from 2 to 12 with almost constant values in the neutral pH range of 6 to 7 (Figure 4d). It was found that maximum DR13 dye removal by NITRS was at pH 6.0 ($q_e = 23 \text{ mg/g}$) with initial concentration of 100 mg/L. Despite the fact, maximum adsorption of the dye was at pH 2, yet we carried out at almost neutral pH, to make it amenable for commercial exploitation. It is clear from (Figure 4d) that as the solution pH increases, the adsorption capacity decreases. Increasing solution pH increases the negatively charged sites, which decreases attraction between the anionic dye DR13 and the biosorbent surface.

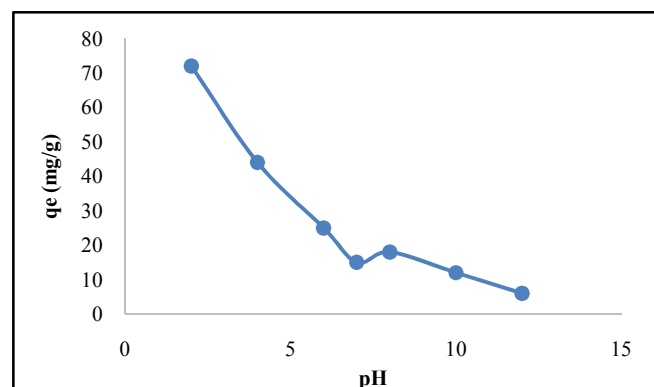


Figure 4 d Effect of pH on adsorption of dye

Effect of Temperature

Temperature is also a factor which influences the adsorption process. The adsorption studies were carried out at 30°C-50°C and the results are shown in Figure 4e. It was observed that with increase in temperature, the adsorption capacity decreased gradually, which indicates that the process is endothermic in nature. The enhancement in adsorption with temperature may be due to the increase in the mobility of the dye molecule with decrease in their kinetic energy and the enhanced rate of intra-particle diffusion phenomenon (Ahmad & Kumar 2010).

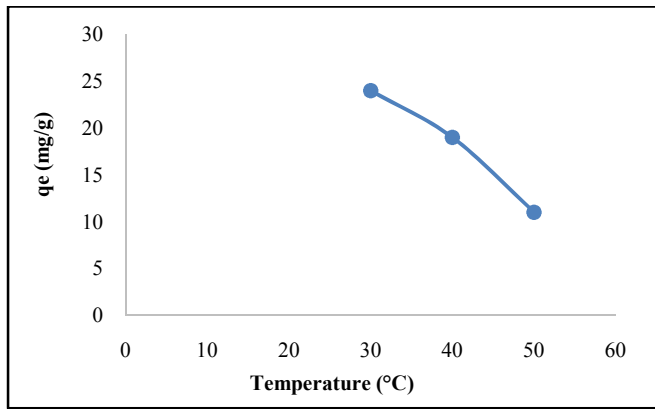


Figure 4e Effect of temperature

Adsorption isotherm

Adsorption isotherm parameters are important for the description of how molecules of adsorbate interact with adsorbent surface. In the present case, an attempt has been made to understand the adsorption of DR13 on to NITRS using different adsorption isotherm models. Langmuir and Freundlich isotherms are the well-established models for predicting the adsorption capacities and can fit the experimental data. The Langmuir isotherm model assumes that the monolayer adsorption takes place on to the surface of adsorbent containing finite number of identical adsorption sites of uniform energies (Langmuir 1916). The Langmuir equation is as shown below:

$$q_e = \frac{Q_m K_a C_e}{1 + K_a C_e} \quad R_L = \frac{1}{1 + K_a C_0} \tag{1}$$

Where, q_e is the amount of dye adsorbed on to adsorbent (mg/g) at equilibrium; C_e is the equilibrium concentration (mg/L) of the dye in solution. The values of Q_m and K_a are determined from the intercept and the slope of q_e vs C_e , where, Q_m is the monolayer adsorption capacity (mg /g) and K_a is the Langmuir constant (L/mg) related to the free energy of adsorption. The equilibrium experiments were conducted for different initial concentrations of DR13 in the range of 25-400 mg/L. The Q_m value of 63.291 mg/g obtained for this isotherm is too high from the experimental value of q_e (23 mg/g). Besides, the value of R^2 of 0.806 shows poor fitting of this isotherm to the experimental data (Figure 5a). Hence it is necessary to explore other adsorption isotherm models.

Freundlich isotherm model is an empirical equation which assumes that the adsorption process takes place on heterogeneous surface (Freundlich 1906). The capacity of adsorption by NITRS is related to the DR13 concentration at equilibrium which follows the equation:

$$q_e = K_F C_e^{1/n_F} \tag{2}$$

Where, K_F and n_F are the Freundlich constants related to adsorption capacity [mg/g and (mg/L)^{-1/n_F}] and adsorption intensity respectively. The latter is also known as the heterogeneity factor (n_F) which indicates whether the nature of adsorption is linear ($n_F=1$), chemisorption ($n_F < 1$), or physisorption ($n_F > 1$). In the present study (Figure 5b), the

value of n_F which is 0.722 indicate that the adsorption is physisorption and favours normal Langmuir Isotherm. The values of K_F and n_F are calculated from the intercept and slope of the plot $\ln q_e$ vs $\ln C_e$. The fitting of Freundlich isotherm to the experimental data has R^2 value of 0.852, where R is the correlation coefficient shows that the process is almost linear. However, it is inferred that the adsorption of DR13 on to NITRS is favourable at experimental conditions and the process is physisorption. To enhance the validity of the results studied, authors have attempt was made to explore Tempkin model to fit in the data.

Tempkin model (Figure 5c) describes the process by considering some indirect adsorbate-adsorbate interactions on adsorption (Amela *et al.*, 2012). This isotherm explains that, the linear decrease in heat of adsorption of all the molecules in the layer is the impact of these interactions. The linear form of Tempkin isotherm is:

$$q_m = (RT/b) \ln A + (RT/b) \ln C_e \tag{3}$$

with $B = RT/b$

Where, q_m is adsorption capacity (mg/g), C_e is equilibrium dye concentration (mg/L). A and B are Tempkin constants, related to equilibrium binding constant (L/g) and heat of adsorption (J/mol), respectively. The values of A and B can be calculated from intercept and slope of the linear plot q_m versus $\ln C_e$. Amongst three models studied, Tempkin isotherm fits better to the experimental data with R^2 value of 0.983, where R is the correlation coefficient and shows that the process is linear. In brief, Langmuir, Freundlich and Tempkin models were used to test the equilibrium adsorption at ambient temperature and the consolidated data are presented in Table 2.

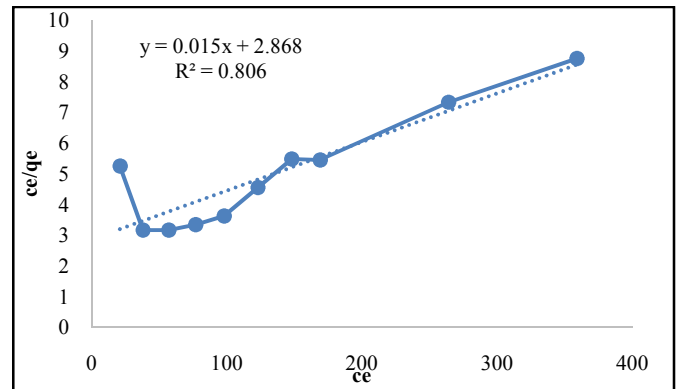


Figure 5 a Langmuir isotherm model

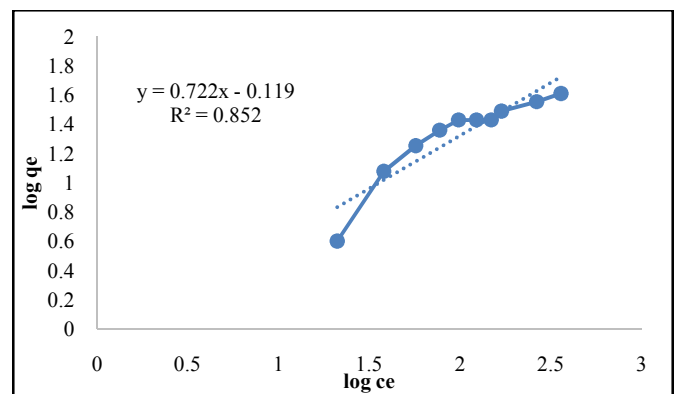


Figure 5 b Freundlich isotherm model

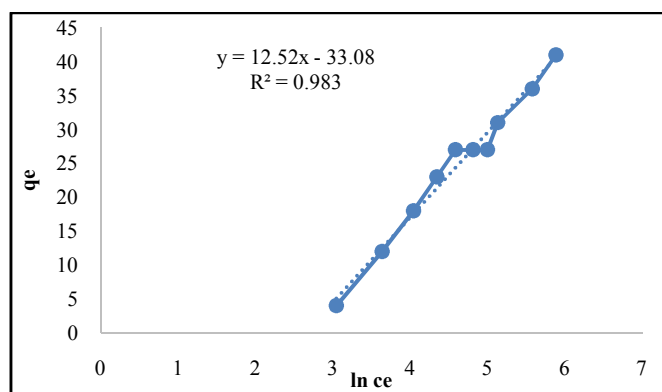


Figure 5 c Tempkin isotherm model

Table 2 Isotherm constants of DR13-NITRS system

Langmuir isotherm		Freundlich isotherm		Tempkin isotherm				
q_m	b	R^2	K_F	n	R^2	A	B	R^2
63	5.507×10^{-3}	0.807	1.317	0.722	0.852	437.52	12.528	0.983

Adsorption Kinetics

In adsorption process, analysis of the kinetic data is important since the kinetics describe the uptake rate of adsorbate which helps to predict the mechanism of adsorption and rate controlling steps. In the present investigation, pseudo-first order and pseudo-second order models have been used for testing the experimental data.

Pseudo-first order kinetic model

The differential rate equation is in the form:

$$dq_t / dt = k_1 (q_e - q_t) \quad (4)$$

where, q_t and q_e are the amounts of dye adsorbed at time t (mg/g) and at equilibrium (mg/g), respectively and k_1 is the pseudo-first order rate constant (min^{-1}). Integrating the above equation using the boundary condition, $q_t = 0$ at $t = 0$.

$$\log (q_e - q_t) = \log q_e - (k_1/2.303) t \quad (5)$$

The values of k_1 and q_e were calculated from the slopes and intercepts of the linear plots of $\log (q_e - q_t)$ versus t respectively and presented in Figure 6a.

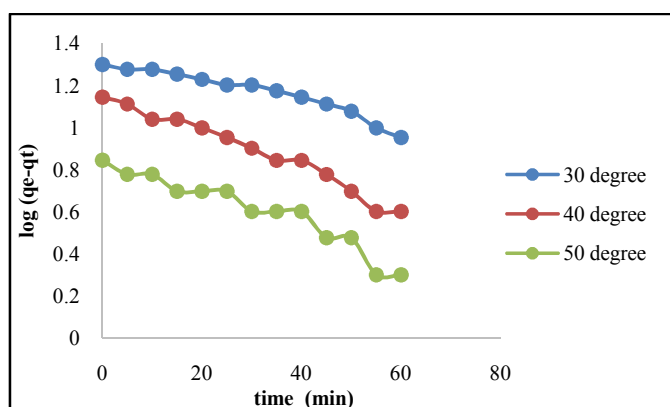


Figure 6a Pseudo-first order kinetic model of DR13 onto NITRS system at different temperatures

Pseudo-second order kinetic model

The pseudo-second order kinetic model is presented as:

$$dq_t / dt = k_2 (q_e - q_t)^2 \quad (6)$$

Where, q_t and q_e are the amount of dye adsorbed at time t (mg/g) and at equilibrium (mg/g), respectively and k_2 is the pseudo-second order rate constant (g/mg min). Integrating the above equation using the boundary condition, $q_t = 0$ at $t = 0$ leads to:

$$t/q_t = 1/k_2^2 q_e^2 + t/q_e \quad (7)$$

The values of k_2 and q_e were calculated from intercepts and slopes of the linear plots of t/q_t versus t (Figure 6b) and presented in Table 3. The values show that the calculated q_e values are very close to that of experimentally obtained q_e and the values of correlation coefficients (R^2) are closer to unity confirms that adsorption of DR13 on NITRS follows pseudo-first order kinetics.

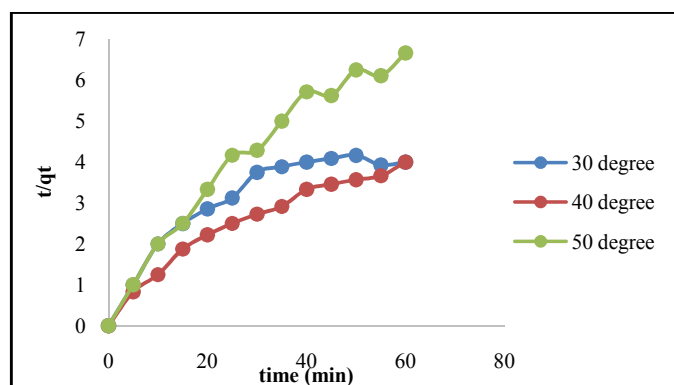


Figure 6 b Pseudo-second order kinetic model of DR13 on NITRS system at different temperatures

Table 3 Experimentally determined and theoretically predicted parameters for absorption kinetics models

Temperature (K)	Initial dye Concentration (mg L^{-1})	q_m exp	Pseudo-first order			Pseudo-second order		
			q_m cal	k_1	R^2	q_m cal	K_2	R^2
303	100	24	21.468	0.0124	0.9297	16.501	3.0450×10^{-3}	0.7935
313	100	19	14.679	0.0211	0.9774	16.583	5.3421×10^{-3}	0.9361
323	100	11	7.272	0.0198	0.9269	9.328	0.0137	0.9505

Statistical optimization by fractional factorial design

Experiments were carried out with different combinations of six independent variables to study the individual as well as combined effects. Analysis of variance (Table 3) obtained from the quadratic regression analysis clearly shows the significance of individual and combined effect of these factors. Significance of factors were considered at confidence interval of 95% with p -value $< 0.05\%$. In this study A, B, C, D, E, F, AB, A², B², C², E² and F² are significant model terms and rest of the variables is insignificant. Cross products AD, AE, BD, BE, BF, CD, CE, CF, DE, DF and EF are zero and hence are excluded to construct the regression equation. The RSM model is highly significant with model F-Value of 147.6. The predicted R^2 value of 0.8317 is in reasonable agreement with the adjusted R^2 value of 0.9641. High R^2 value of 97.1% with insignificant lack of fit and high coefficient of variance (CV) of 20% assure that model can be used to navigate the design space. The comparison graph for actual versus predicted values (Figure 7) indicate a strong relationship between the experimental and predicted responses. The regression equation obtained from the study is shown below equation (Equation 8)

$$\text{Adsorption} = 14.8 + 7.0 * A - 2.3 * B + 11.5 * C + 4.3 * D - 10.9 * E - 30.9 * F - 3.3 S * AB - 4.4 * A^2 - 3.9 * B^2 - 16.8 * C^2 + 0.3 * D^2 + 9.4 * E^2 - 17.0 * F^2 \quad (8)$$

Design-Expert® Software
 Color points by value of
 qe(mg/g):
 72
 4

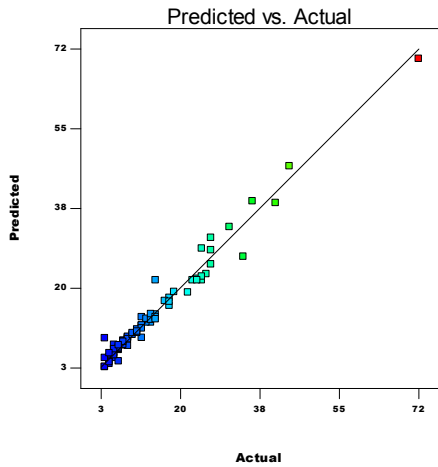


Figure 7 Comparison graph for actual versus predicted values

Table 4 ANOVA for Fractional factorial design

Source	Sum of Squares	Degree of freedom	Mean Square	F Value	P- Value
Model	9139.1	13	703.0	147.6	< 0.001**
A	681.2	1	681.2	143.0	< 0.001**
B	105.8	1	105.8	22.2	< 0.001**
C	175.7	1	175.7	36.9	< 0.001**
D	76.6	1	76.6	16.1	< 0.001**
E	509.8	1	509.8	107.0	< 0.001**
F	2678.4	1	2678.4	562.3	< 0.001**
AB	113.8	1	113.8	23.9	< 0.001**
A^2	78.1	1	78.1	16.4	< 0.001**
B^2	91.8	1	91.8	19.3	< 0.001**
C^2	143.8	1	143.8	30.2	< 0.001**
D^2	0.1	1	0.1	0.0	0.9056
E^2	101.0	1	101.0	21.2	< 0.001**
F^2	552.6	1	552.6	116.0	< 0.001**
Residual	276.3	58	4.8		
Lack of fit	213.5	55	3.9	0.2	0.9975
Total	9415.3	71			

Significant figures
 + Suggestive significance (p value: 0.05 < p < 0.10)
 * Moderately significant (p value: 0.01 < p ≤ 0.05)
 ** Strongly significant (p value: p ≤ 0.01)

The optimal values of the variables determined by maximization of the second-order polynomial equation with interaction terms obtained by multiple regression analysis based on CCD. Maximum adsorption obtained by the statistical optimization experiment was 108mgg⁻¹ with optimized conditions established as a pH of 1, adsorbent dosage of 0.03 g L⁻¹ and an initial dye concentration of 325 mg L⁻¹ for an adsorption time of 179 min with orbital shaking of 165 rpm at temperature 29°C.

The last step of the statistical optimization was the analysis of the 3D response surface plots and contour plots as a function of two independent variables, which served the purpose of determining the interaction effects between two parameters keeping the others at a fixed value. Statistical process optimization, in a given range of parameter values, allows not only for calculating the optimal condition, but also for determining the effect of the process conditions on the adsorption. 3D graphs (Figures 8-13) plotted for time against all other factors indicate that time has a positive effect on

adsorption capacity. By increasing time along with particle size and dye concentration, we can increase the process of adsorption. Maximum time of 180 min has shown maximum adsorption. Increase in temperature beyond 30 °C has negative effect on adsorption capacity. As temperature increases adsorption capacity decreases. Increase in pH beyond 1 decreases adsorption capacity even if time is increased. Graph (Figure 11) plotted against time and adsorbent dosage indicates that adsorbent dosage has negative effect on adsorption; however, increased time can improve the process of sorption. Graphs (Figures 13-16) for temperature against other independent variables indicate that temperature has negative effect with all other variable on the response. Graphs (Figures 17-19) plotted for initial dye concentration against other variables indicate that increase in the initial concentration have positive effect for adsorption capacity. The values of the regression coefficients, in seen equation 1, indicate the effect the parameter has on the adsorption capacity. Positive values indicate incremental effect, for example, an increase in the Time (A) causes a significant increase in sorption capacity.

Likewise, a negative value indicates a detrimental effect, as seen in the case of pH (F), i.e., an increase in pH decreases the adsorption capacity of the adsorbent. Thus effect of two parameters together on the biosorption is graphically represented in the surface and contour plots (Fig.8-22).

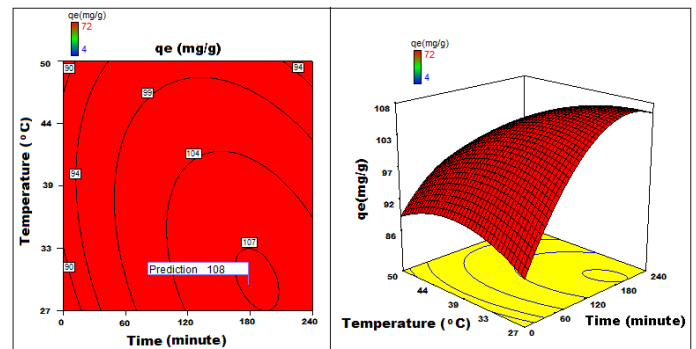


Figure 8 3D surface plot and contour plot showing the variation of adsorption capacity with temperature versus time

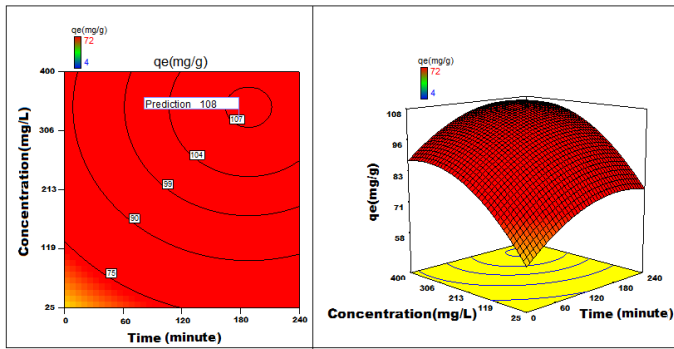


Figure 9 3D surface plot and contour plot showing the variation of adsorption capacity with time versus concentration

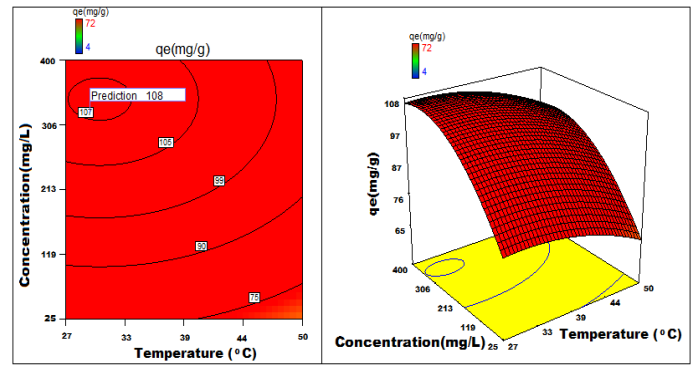


Figure 13 3D surface plot and contour plot showing the variation of adsorption capacity with temperature versus concentration

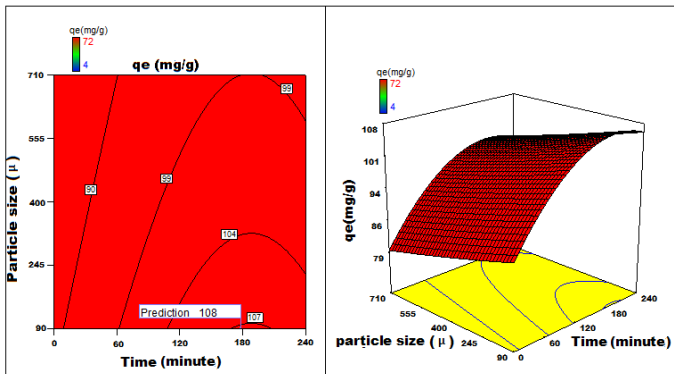


Figure 10 3D surface plot and contour plot showing the variation of adsorption capacity with time versus particle size

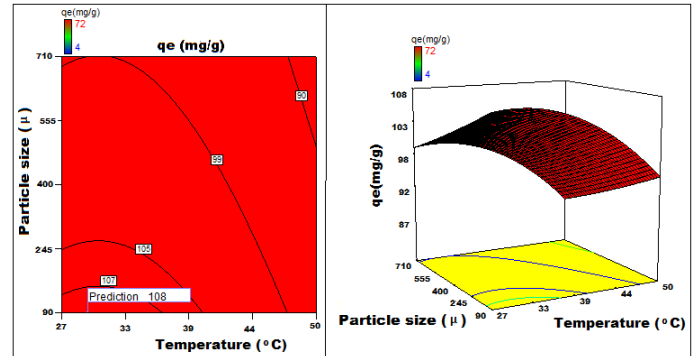


Figure 14 3D surface plot and contour plot showing the variation of adsorption capacity with temperature versus orbital particle size

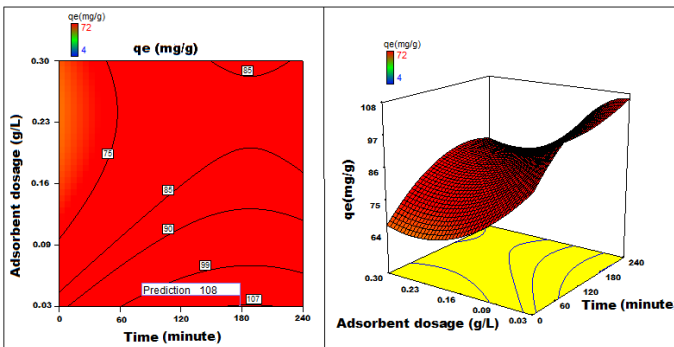


Figure 11 3D surface plot and contour plot showing the variation of adsorption capacity with time versus adsorbent dosage

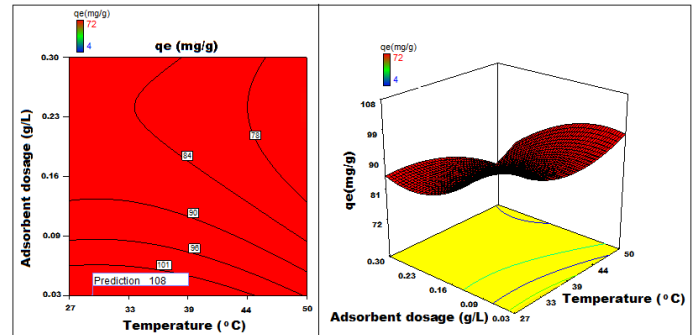


Figure 15 3D surface plot and contour plot showing the variation of adsorption capacity with temperature versus adsorbent dosage

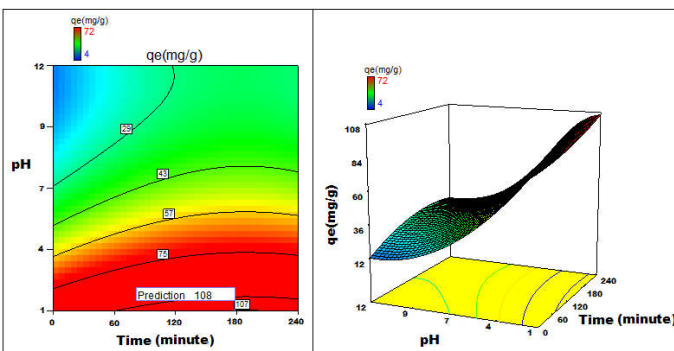


Figure 12 3D surface plot and contour plot showing the variation of sorption capacity with time versus pH

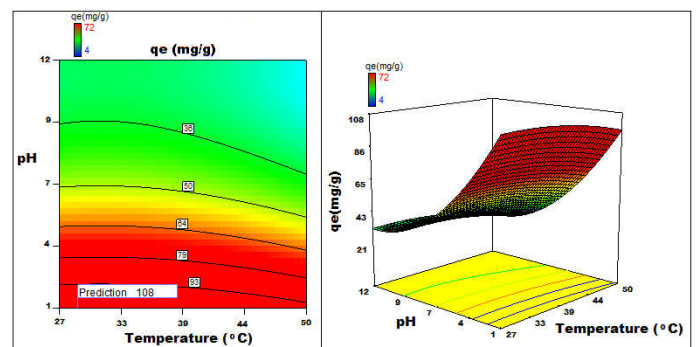


Figure 16 3D surface plot and contour plot showing the variation of adsorption capacity with temperature versus pH

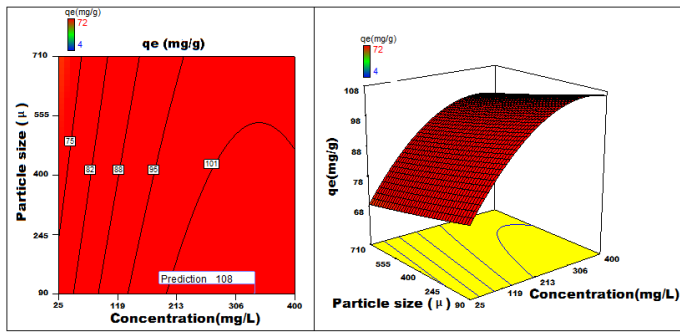


Figure 17 3D surface plot and contour plot showing the variation of adsorption capacity with particle size versus concentration

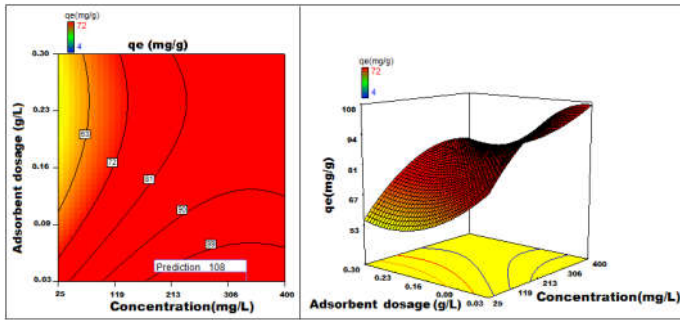


Figure 18 3D surface plot and contour plot showing the variation of adsorption capacity with adsorbent dosage versus concentration

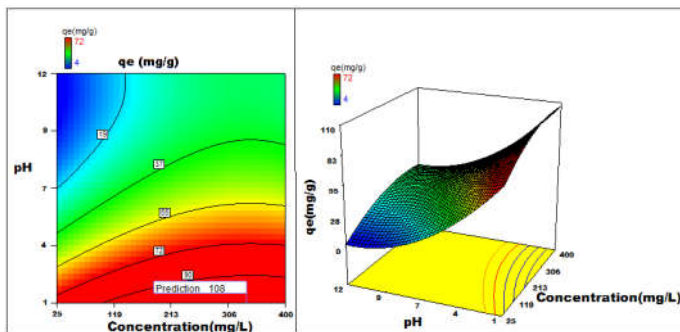


Figure 19 3D surface plot and contour plot showing the variation of adsorption capacity with pH versus concentration

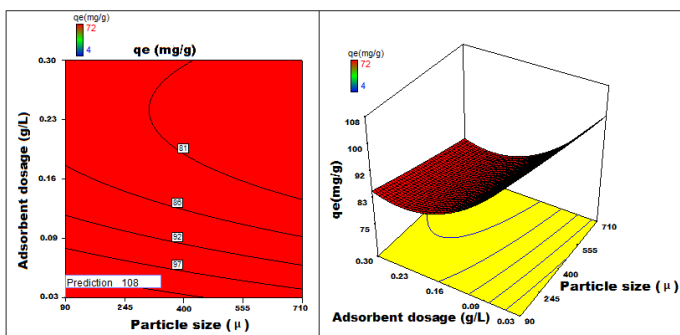


Figure 20 3D surface plot and contour plot showing the variation of adsorption capacity with adsorbent dosage versus particle size

The quadratic model developed for process optimization is found to be beneficial for predicting the maximum adsorption capacity and understanding the interaction between independent variables as well as their effect on adsorption process. From statistical optimization there is almost 66.7% increase in adsorption from 72 mg g^{-1} to 108 mg g^{-1} .

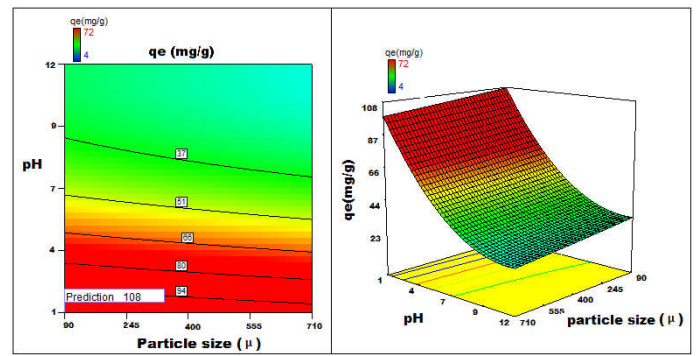


Figure 21 3D surface plot and contour plot showing the variation of adsorption capacity with pH versus particle size

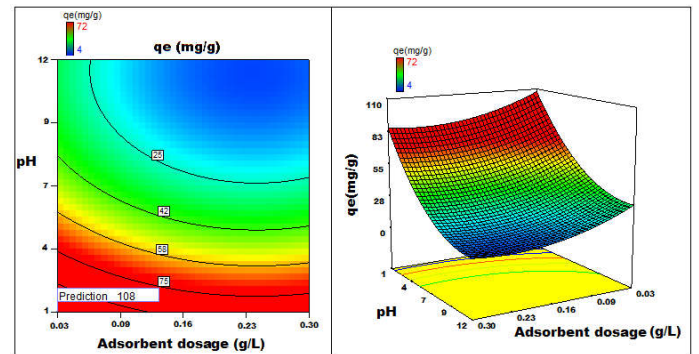


Figure 22 3D surface plot and contour plot showing the variation of adsorption capacity with adsorbent dosage versus pH

Regeneration of the adsorbent and cost analysis Regeneration of dye adsorbed NITRS enables its re-use and also it is necessary to recover the adsorbed dye. The cost of the entire process including cost of solvent cost for recovering of the adsorbent may exceed the total cost of the adsorbent and the dye. Hence it is not feasible proposition. It will enhance the E-factor which is undesirable to the planet earth. In view of increased stringencies imposed to restrict pollution, a novel approach has been made in our research school to use the dye adsorbed biosorbent as a filler material in the fabrication of thermoplastics and thermosets.

CONCLUSION

The adsorption of DR13 from aqueous solution by NITRS is dependent on contact time, initial pH of the solution, adsorbent dose and initial dye concentration. Based on isotherm analysis and considering the Q_m value, the adsorption by NITRS is well described by Tempkin isotherm model, and the adsorption kinetics fitted well to pseudo-first order kinetics model. The optimal values of the variables determined by maximization of the second-order polynomial equation with interaction terms obtained by multiple regression analysis based on a central composite experimental design model and the input parameters, the predicted adsorption capacity of NITRS under optimal conditions ranged from 72 mg g^{-1} to 108 mg g^{-1} .

The major observations of this study include:

- NITRS is an efficient, environmental-friendly and cost-effective biosorbent for the remediation of toxic Direct Red 13 dye.
- Various parameters including initial dye concentration, adsorbent dose, and its particle size, temperature and pH

of the medium influenced the adsorption efficiency of NITRS.

- The results proved that maximum efficiency of adsorption occurred at pH 2. Nevertheless, the neutral pH proved most cost effective.
- The experimental results of the adsorption isotherms and kinetic studies confirmed the complexity involved in the dye adsorption.
- Spontaneous and endothermic nature of biosorption was evident and the adsorption was of physical in nature.
- This alternative use of NITRS as a biosorbent will help to reduce carbon foot print.
- This concept and approach will help in preventing resource depletion through utilization of agro-based spent which has otherwise neither feed or fertilizer value.
- The work is academically interesting and commercially achievable.

Acknowledgment

One of the authors (MAHDA) gratefully acknowledges Tamar University, Republic of Yemen for the award of Overseas Research Fellowship.

References

- Ahmad, R. & Kumar, R. (2010). Adsorption studies of hazardous malachite green onto treated ginger waste. *Journal of Environmental Management*, 91(4), 1032-1038.
- Amela, K., Hassen, M. A. & Kerroum, D. (2012). Isotherm and kinetics study of biosorption of cationic dye onto banana peel. *Energy Procedia*, 19, 286-295.
- Bafana, A., Devi, S. S., & Chakrabarti, T. (2011). Azo dyes: past, present and the future. *Environmental Reviews*, 19, 350-371.
- Freundlich, HMF. (1906). Over the adsorption in solution. *Journal of Physical Chemistry*, 57, 385-471.
- Falkenmark, M. (2003). Freshwater as shared between society and ecosystems: from divided approaches to integrated challenges. *Philosophical Transactions of the Royal Society B: Biological Sciences*, 358(1440), 2037-2049.
- Glenn, J. C., Gordon, T. J., & Florescu, E. (2014). State of the future. *Washington, DC: The Millennium Project*. <https://globenewswire.com/news-release/2017/03/10/934428/0/en/285-Billion-Nutraceuticals-Industry-Report-Global-Market-Data-from-2015-Estimates-for-2016-Projections-to-2021.html>.
- Hubbe, M. A., Hasan, S. H., & Ducoste, J. J. (2011). Cellulosic substrates for removal of pollutants from aqueous systems: A review. 1. Metals. *Bio Resources*, 6(2), 2161-2287.
- Joe, B., Vijaykumar, M., & Lokesh, B. R. (2004). Biological properties of curcumin-cellular and molecular mechanisms of action. *Critical Reviews in Food Science and Nutrition*, 44(2), 97-111.
- Langmuir, I. (1916). The constitution and fundamental properties of solids and liquids. *Journal of the American Chemical Society*, 38(11), 2221-2295.
- Papegowda, P. K., & Syed, A. A. (2017). Isotherm, Kinetic and Thermodynamic Studies on the Removal of Methylene Blue Dye from Aqueous Solution Using Saw Palmetto Spent. *International Journal of Environmental Research*, 11(1), 91-98.
- Pashaei, S., Siddaramaiah, & Syed, A. A. (2011). Investigation on mechanical, thermal and morphological behaviors of turmeric spent incorporated vinyl ester green composites. *Polymer-Plastics Technology and Engineering*, 50(12), 1187-1198.
- Sheldon, R. A. (1992). Organic synthesis-past, present and future. *Chemistry and Industry*, 23, 903-906.
- Sulthana, R., Taqui, S.N., Zameer, F., Taqui, S.U., and Syed, A.A. (2017). Adsorption of ethidium bromide from aqueous solution on to nutraceutical industrial fennel seed spent: Kinetics and thermodynamics modeling Studies. *International journal of phytoremediation*, doi 10.1080/15226514.2017.1365331.
- Syed, M. A., Siddaramaiah, Suresha, B., & Syed, A. A. (2009). Mechanical and abrasive wear behavior of coleus spent filled unsaturated polyester/polymethyl methacrylate semi interpenetrating polymer network composites. *Journal of Composite Materials*, 43(21), 2387-2400.
- Syed, M. A., Ramaraj, B., Akhtar, S., & Syed, A. A. (2010). Development of environmentally friendly high density polyethylene and turmeric spent composites: Physicomechanical, thermal, and morphological studies. *Journal of Applied Polymer Science*, 118(2), 1204-1210.
- Syed, M. A., Siddaramaiah, Syed, R. T., & Syed, A. A. (2010a). Investigation on Physico Mechanical Properties, Water, Thermal and Chemical Ageing of Unsaturated Polyester/Turmeric Spent Composites. *Polymer-Plastics Technology and Engineering*, 49(6), 555-559.
- Syed, M. A., Akhtar, S., & Syed, A. A. (2011). Studies on the physic mechanical, thermal and morphological behaviors of high density polyethylene/coleus spent green composites. *Journal of Applied Polymer Science*, 119(4), 1889-1895.
- Syed, M. A., & Syed, A. A. (2012). Development of a new inexpensive green thermoplastic composite and evaluation of its physico-mechanical and wear properties. *Materials & Design (1980-2015)*, 36, 421-427.
- Syed, M. A., & Syed, A. A. (2016). Development of green thermoplastic composites from Centella spent and study of its physicomechanical, tribological, and morphological characteristics. *Journal of Thermoplastic Composite Materials*, 29(9), 1297-1311.
- Syed, M. A., & Syed, A. A. (2016a). Investigation on physicomechanical and wear properties of new green thermoplastic composites. *Polymer Composites*, 37(8), 2306-2312.
- Taqui, S. N., Yahya, R., Hassan, A., Nayak, N., & Syed, A. A. (2017). Development of sustainable dye adsorption system using nutraceutical industrial fennel seed spent—

- studies using Congo red dye. *International Journal of Phytoremediation*, 19(7), 686-694.
- Unnithan, M. R., & Anirudhan, T. S. (2001). The kinetics and thermodynamics of sorption of chromium (VI) onto the iron (III) complex of a carboxylated polyacrylamide-grafted sawdust. *Industrial & engineering chemistry research*, 40(12), 2693-2701.
- Yao, Z., Wang, L., & Qi, J. (2009). Biosorption of methylene blue from aqueous solution using a bioenergy forest waste: *Xanthocerasorbifolia* seed coat. *CLEAN-Soil, Air, Water*, 37(8), 642-648.
- Zaffalon, V. (2010). Carbon mitigation and textiles. *Textile World*, 35.

How to cite this article:

Mohammed A. H.Dhaif Allah and Akheel Ahmed Syed.2018, Development of Sustainable Dye Adsorption System Using Nutraceutical Industrial Turmeric Root Spent-Studies With Direct Red 13. *Int J Recent Sci Res.* 9(2), pp. 24370-24380.
DOI: <http://dx.doi.org/10.24327/ijrsr.2018.0902.1649>
